Journal of Dynamics, Monitoring and Diagnostics, 2023, 2, 190-197
https://doi.org/10.37965/jdmd.2023.159

ISTP
RESEARCH ARTICLE

Smart Monitoring of Solar Photovoltaic Panels by the Approach of Machine Learning

Xing Wang,[1] Wenxian Yang,[2] and Jinxin Wang[3]
[1]Estun Automation Co. Ltd, Nanjing 211102, China
[2]School of Engineering, Newcastle University, Newcastle upon Tyne NE1 7RU, UK
[3]School of Safety Engineering, China University of Mining and Technology, Xuzhou 221116, China

(Received 06 February 2023; Revised 06 September 2023; Accepted 12 September 2023;
Published online 12 September 2023)

Abstract: The exploitation of renewable energy has become a pressing task due to climate change and the recent energy crisis caused by regional conflicts. This has further accelerated the rapid development of the global photovoltaic (PV) market, thereby making the management and maintenance of solar photovoltaic (SPV) panels a new area of business as neglecting it may lead to significant financial losses and failure to combat climate change and the energy crisis. SPV panels face many risks that may degrade their power generation performance, damage their structures, or even cause the complete loss of their power generation capacity during their long service life. It is hoped that these problems can be identified and resolved as soon as possible. However, this is a challenging task as a solar power plant (SPP) may contain hundreds even thousands of SPV panels. To provide a potential solution for this issue, a smart drone-based SPV panel condition monitoring (CM) technique has been studied in this paper. In the study, the U-Net neural network (UNNN), which is ideal for undertaking image segmentation tasks and good at handling small sample size problem, is adopted to automatically create mask images from the collected true color thermal infrared images. The support vector machine (SVM), which performs very well in high-dimensional feature spaces and is therefore good at image recognition, is employed to classifying the mask images generated by the UNNN. The research result has shown that with the aid of the UNNN and SVM, the thermal infrared images that are remotely collected by drones from SPPs can be automatically and effectively processed, analyzed, and classified with reasonable accuracy (over 80%). Particularly, the mask images produced by the trained UNNN, which contain less interference items than true color thermal infrared images, significantly benefit the assessing accuracy of the health state of SPV panels. It is anticipated that the technical approach presented in this paper will serve as an inspiration for the exploration of more advanced and dependable smart asset management techniques within the solar power industry.

Keywords: condition monitoring; neural network; solar photovoltaic panels; support vector machine

I. BACKGROUND

The solar photovoltaic (SPV) market is booming globally. For example, the power generation from SPV increased by 179 TWh in 2021, marking an increase of 22% over 2020. Today, global solar PV generation has exceeded 1000 TWh, accounting for 3.6% of global electricity generation. This makes solar power the third largest renewable power technology behind hydropower and wind. Of the total growth of solar power generation in 2021, China contributes about 38%. The second largest growth, 17%, occurred in the United States, and the third largest growth, 10%, was in the European Union [1]. However, the average annual generation growth of 25% in the period of 2022 to 2030 is needed to follow the Net Zero Emissions by 2050 Scenario [2]. This corresponds to a more than threefold increase in annual capacity deployment until 2030. That means, the future annual solar PV capacity addition will be about 600 GW. Since single SPV panel in the current market is rated at 1∼4 kW, the capacity addition of 600 GW means that 150∼600 million solar PV panels will be newly installed every year. This will raise a challenging asset management issue in solar power plants (SPP). Although SPV panels are generally considered to be reliable and low maintenance, there is still a possibility that issues may arise during the various stages of their production, transportation, and installation. These problems could potentially affect the performance or lifespan of the SPV panels. They also face many risks during the long service life, which may degrade their power generation performance [3,4]. Therefore, in the solar power industry today, the task of promptly identifying faulty SPV panels from hundreds of them and furthermore accurately diagnosing the fault has become a crucial challenge. To address this issue, much effort has been made in the past years [4–11]. The currently available techniques can be roughly categorized into two categories. The first category of technique, such as those reported in [4,5], was developed for analyzing the electrical signals output from the SPV panels. They assess the panel's health condition by comparing the collected electrical signals with the historical signals collected from healthy panels. The second category of technique, such as those reported in [9,10], relies on investigating the features of the images taken from the SPV panels. They judge the panel's health state by detecting the abnormal changes in image features using image processing and classification methods. Such research, particularly the work reported in [9,10], was developed based on a

Corresponding author: Wenxian Yang (e-mail: Wenxian.yang@newcastle.ac.uk).

hypothesis, i.e., the presence of a fault in SPV panel will result in temperature change in the defective area, and therefore can be detected by a thermal infrared camera or other temperature measurement means. Since different types of SPV panel faults are caused by different components in the system, they show distinct appearances in images. Therefore, it is realistic to roughly judge the types of SPV panel faults through observing the fault-related features of the images. In comparison,

- The first category of technique is usually considered ideal for online monitoring a small number of individual SPV panels as it involves simple hardware configuration and calculation. However, it will face a challenge when applied to monitor a huge number of panels due to the significantly increased cost and complexity of the hardware.
- The second category of technique is more economical when applied to simultaneously monitor hundreds of SPV panels in a SPP as it does not require using lots of transducers and the associated hardware. Since the images of solar PV panels can be readily collected using drones, the second category of technique is attracting increasing interest today from both scholars and industrialists.

However, how to process the collected PV panel images quickly and effectively and apply them to the in situ asset management in the SPP is still a technology gap. The work reported in this paper is a part of the contribution to address this technology gap. The novelty of this paper is that a smart health state assessment method will be developed specifically for SPV panels solely based on intelligent processing and analysis of the thermal infrared images. The corresponding algorithms will be developed with the aid of the U-Net neural network (UNNN) and support vector machine (SVM).

The reason for adopting the UNNN and SVM in this study is based on their numbers of key advantages in image processing and image classification. For example, the UNNN is a specialized convolutional neural network (CNN) commonly used for image segmentation tasks. It was designed for pixel-wise semantic segmentation, which means it can accurately identify and segment objects or regions of interest within an image. Moreover, the UNNN consists of an encoder path and a decoder path. The encoder gradually reduces spatial resolution while increasing the number of channels to capture high-level features, and the decoder path upscales the feature maps to produce a segmentation mask. This architecture enables precise localization of object boundaries [11]. In the past years, it has been successfully applied to tumor segmentation in medical images, road detection in satellite imagery, and cell nucleus segmentation in microscopy images. It is believed that the UNNN can continue its success in processing the thermal infrared images in this study. The SVM performs well in high-dimensional feature spaces, which is especially useful when dealing with data that has many features. This makes it suitable for tasks like text classification, image recognition, and genomics. In addition, the SVM is less prone to overfitting and less affected by outliers compared to many other machine learning algorithms [12]. These advantages will significantly benefit the accuracy of classification when applied to assess the health state of SPV panels.

The rest of the paper is organized as follows. To ease understanding, Section II will give a brief introduction to the three popular types of SPV panel faults that may occur in the practice of solar power generation. Section III will introduce the method used for image collection. To develop the database for performing machine learning, image processing and image sample expansion methods will be developed in Section IV. The method for extracting features from thermal infrared images will be developed in Section V. A smart SPV panel condition monitoring (CM) technique will be developed and tested in Section VI. Finally, the paper is ended in Section VII with a few key conclusions.

II. POPULAR SPV PANEL FAULTS

The long-term practice has shown that SPV panels may develop faults during the process of manufacturing, transport, and installation. They may also fail during the subsequent power generation process due to harsh environments, grid problems, or other unforeseen reasons [13,14]. Since faults can cause optical degradation or electrical mismatch of the SPV panels [15], the efficiency of the SPV panels will decrease significantly in the presence of a fault. So, it is hoped that these faults can be identified and resolved as soon as they are present to avoid significant economic losses or secondary damage to other facilities in the SPP. Although various types of faults may develop in SPV panels, the most popular types of faults are power unit faults, safety glass cracks, and safety glass contaminations [16,17]. To facilitate understanding, the thermal infrared images in the presence of these three types of faults are shown in Fig. 1. In the figure, the color indicates the relative temperature in the surface area of the SPV panels.

From Fig. 1, it is seen that completely different graph features can be observed from the thermal infrared images when different types of faults are developed in the solar PV

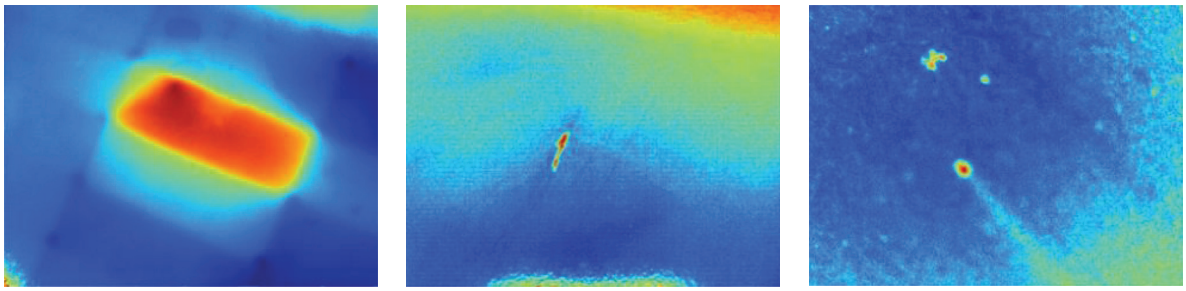

(a) Power unit fault (b) Safety-glass crack (c) Safety-glass contaminations

Fig. 1. Three popular types of faults occurring in solar PV panels.

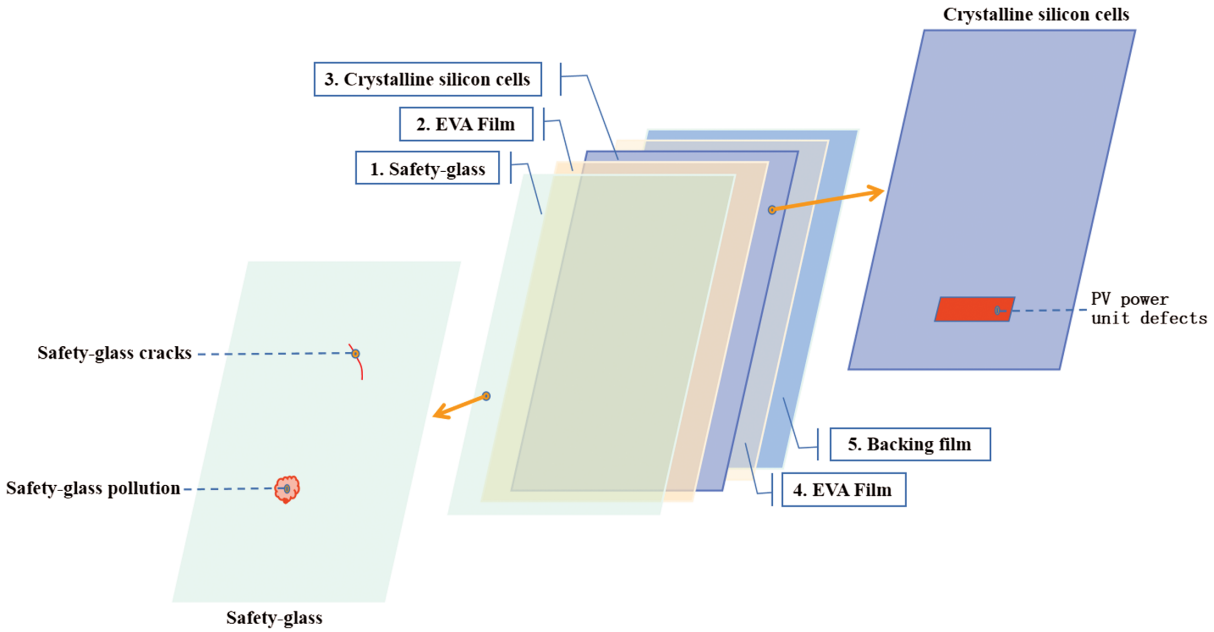

Fig. 2. The structural configuration of a solar PV panel [15].

panels. This suggests the feasibility of identifying and diagnosing SPV panel faults by analyzing the thermal infrared images remotely taken from the SPV panels by a drone. To help understand the three popular types of SPV panel faults, Fig. 2 shows the structural configuration of a solar PV panel.

Of the three popular types of faults, power unit failure is usually resulted by mechanical damage during manufacturing, installation, and transportation. Faults of this type can result in power failure or lead to the failure of some function modules, with a noticeable temperature change in the vicinity of the faults. The cracking of safety glass may occur due to improper handling during manufacturing, installation, and transportation, as well as due to shocks and extreme temperature. Usually, once the safety glass breaks, the SPV panels may display signs of delamination, air bubbles, discoloration of the encapsulating material, and cracked PV glass. In practice, the detection of such type of fault depends on the sensitivity of the detection methods and tools to the fault. Usually, this type of fault can result in a local temperature increase at the location of the fault and a 4–10% power generation loss. The pollution of safety glass may be caused by the dust on the surface of the SPV panel, the accumulation of bird droplets or other dirt. As a consequence of this type of fault, the temperature in the vicinity of contamination will change abnormally, causing a decrease in the efficiency of the SPV panels.

III. IMAGE COLLECTION

In this study, a thermal imaging camera, modeled FLUKE Ti 450, was employed to collect the thermal infrared images of the SPV panels. It is shown in Fig. 3, and its specifications are listed in Table I.

In the study, in order to develop a smart machine learning network for diagnosing SPV panel faults, a database will be established first, in which the thermal infrared

Fig. 3. Thermal imaging camera FLUKE Ti450 [15].

images collected from the SPV panels in the following four health states will be considered:

(a) Healthy SPV panels

(b) SPV panels with cracks on safety glass

(c) SPV panels with power unit failure

(d) SPV panels with polluted safety glass

The specifications of the solar PV panels used for this study are listed in Table II.

During the collection of images, all images of SPV panels were taken using a FLUKE Ti450 camera without interruption of the panel's operation despite their health states. The thermal infrared camera was set up 0.6–1.0 m above the SPV panels to mimic a scenario in which the camera is carried by a drone to monitor the panels. Since the assessment of the health state of SPV panels relies on characterizing the graph features within the images rather than the size of patterns, the variation in camera distance above the SPV panels and camera shooting angle should not

Table I. Technical specifications of the camera [15]

Characteristics	
IFOV with standard lens (spatial resolution)	1.31mRad, D:S 753:1
Detector resolution	320 × 240
Multi-Sharp™ Multi-point focus	Close and telephoto images can be captured in the whole view.
Laser rangefinders	Yes, calculate the distance to the target to obtain a precisely focused image.
Temperature measurement	
Temperature measurement range	−20~1200°C(−4~2192°F)
Accuracy	±2°C at a nominal temperature of 25°C
Thermal sensitivity (NETD)	≤0.05°C (50 mK), target temperature 30°C

Table II. Specifications of the solar PV panel used in the study [15]

Maximum power	110 W
Maximum operating voltage	18 V
Maximum operating current	6.11 A
Open-circuit voltage	23.66 V
Short-circuit current	8.4 A

affect the assessment results. In the experiment, a total of 295 images were taken, of which 98 images were from the panels in the type (a) health state, 73 were from the panels in the type (b) health state, 64 from the panels in type (c) health state, and 60 from the panels in type (d) health state, respectively.

IV. IMAGE PROCESSING AND IMAGE SAMPLE EXPANSION FOR DATABASE ESTABLISHMENT

In order to facilitate image storage and processing, the software SmartView was adopted firstly to convert the collected image into real color images with 24-bit depth and 320 × 240 resolution. Since the UNNN has a capability to tackle the problem of limited sample availability in image segmentation [18], it will be adopted in this study and trained for automatically generating the mask images from the true color images that are newly obtained using SmartView. Since the mask images contain fewer interference information than true color images, the application of mask images can help increase the accuracy of image classification. To obtain correct mask images required by the training of the UNNN, software LabelMe will be used to process the true color images. To ensure the accuracy of the mask images, the defect areas on the true color image are outlined with the aid of the software LabelMe during the mask image creation process. To ease understanding, the mask images obtained using SmartView and LabelMe from the three true color images in Fig. 1 are shown in Fig. 4. Where, the images are 320 × 240 black images. Herein, it is worth noting that all pixel values in the mask image of a healthy SPV panel will be set to 0.

By comparing Figs. 1 and 4, it is seen that that all the interference items in true color images have disappeared in the corresponding mask images. Undoubtedly, this will be very helpful to improve the accuracy of CM and fault diagnosis of SPV panels.

Even though the UNNN can handle small sample size problem, the use of more training samples can still enhance the quality of image segmentation. In the study, three methods were also adopted in the following to expand the database of image samples. They are (1) mirroring (i.e., creating a new image by flipping the original image left and right), (2) flipping (i.e., creating a new image by flipping the original image up and down), and (3) cropping and zooming in (i.e., creating a new image by cropping and zooming in the original image), respectively. To ease understanding, a few examples of the new images generated using these three image sample expansion methods are illustrated in Fig. 5. In the figure, all four new images were generated from an original safety glass crack image.

To generate more image samples for training the UNNN, the corresponding mask images also need to be expanded using the aforementioned image sample expansion methods. In the end, a total of 2,352 mask images are obtained in the database, of which 1,852 are for training the UNNN, and the rest will be used for verification.

(a) Power unit fault (b) Safety-glass crack (c) Safety-glass contaminations

Fig. 4. The mask images that correspond to the true color images in Fig. 1.

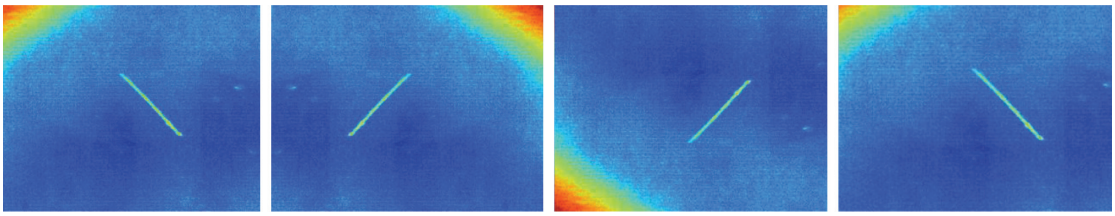

(a) Original image (b) Result of mirroring (c) Result of flipping (d) Result of cropping

Fig. 5. An example of image sample expansion.

V. IMAGE FEATURE EXTRACTION

Since mask images contain less interference items and this benefits the accuracy of monitoring and diagnosing SPV panels, a UNNN will be trained in this section to automatically produce mask images from the true color images. The UNNN training process is illustrated in Fig. 6.

As shown in Fig. 6, the UNNN algorithm is implemented by two tools, i.e., encoder and decoder. The encoder is responsible for extracting features from the true color images by reducing their resolution four times. The decoder is responsible for increasing the resolution of the extracted features back to the original true color image size by the approach of up-sampling. Then, the image segmentation results can be readily obtained by calculating the probability of each pixel. In this study, the UNNN training algorithm is coded in Python 3.7. The Python codes are shown in Fig. 7.

In the UNNN training process, the similarity between the image created by the trained UNNN and real mask image is measured by a Dice coefficient, of which the value varies in the range of [0, 1]. The larger the value of the Dice coefficient, the more similar the newly created image is to the real mask image. The Dice coefficient is expressed as:

$$\text{Dice} = \frac{2 \times (\text{pred} \cap \text{true})}{\text{pred} \cup \text{true}} \tag{1}$$

where "pred" denotes the predicted values and "true" denotes the true values. The symbol "∩" refers to the operation of the dot product and the symbol "∪" represents the operation of the linear sum of the pixel values in the output image and the real mask image.

By using the trained UNNN, the mask images corresponding to the true color thermal images can be generated quickly and correctly. Some of the results are shown in Fig. 8.

From Fig. 8, it is found that when different types of faults occur in the SPV panels, the defective areas in the mask images exhibit distinct graph contour features. Specifically, when the SPV panel has a power unit fault, a regular-shaped contour with a large area and long perimeter is present. If there is a crack on the safety glass surface, a slender-shaped contour can be seen from the mask images. An irregular-shaped contour is often associated with contamination of the safety glass by dust, dirt, or shadows. If the SPV panel is healthy and defect-free, no white graph will be present in the mask images. Herein, it is important to acknowledge that all the aforementioned fault-related image features were observed only in the context of this study. However, it is essential to recognize that these observations may exhibit variations in real-life SPV applications owing to a multitude of factors. To facilitate the description of these fault-related image features, the area and the perimeter of the graph contour were used firstly to characterize the mask images. This is because Fig. 8 shows that the fault-related features exhibit different geometric shapes and sizes when the SPV panels are under different health conditions. Besides, "aspect ratio" and "the ratio of contour area to the area of the outer rectangle" of the

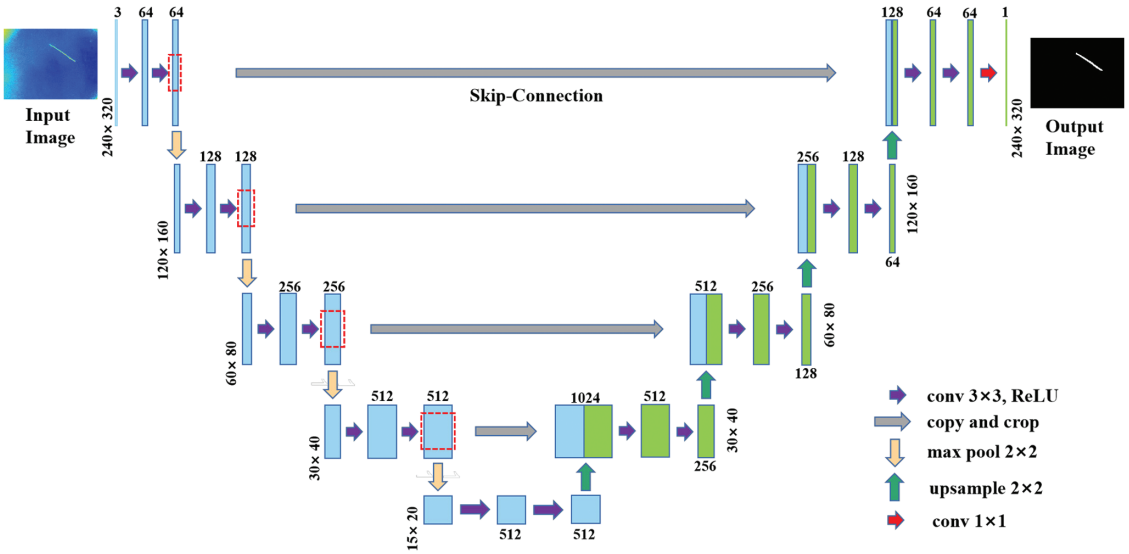

Fig. 6. The working process of a UNNN [13].

```
//I1 is the image used for segmentation training in the training database I
//I2 is the image used for Dice evaluation in I
  input: I = {I1, I2}
  output: O  //As the parameters of the UNNN obtained from the segmentation
             //training
  epoch = 200
  batch size ← {4,6,8,10,12}
  learning rate ← {1×10-2,1×10-3,1×10-4,1×10-5,1×10-6}
  optimizer←RMSprop
  scheduler←ReduceLROnPlateau
  criterion←BCEWithLogitsLoss
  I_train, I_val←Normalization(I1, I2)  //Normalization pre-processing of the input image
  for epoch = 0:200
    //Take batch-size images from I_train one at a time and input them into the network
    for batch∈I_train(batch size)
      Mp←UNNN .train(batch)  //Mp is the prediction mask image output by the UNNN
                             //algorithm
      loss←criterion(Mp, Mt)  //Mt is a true mask image
      optimizer.zero_grad()  //Gradient clearing
      loss.backward()  //Backpropagation calculation to obtain gradient values
      clip_grad_value_(U-Net .parameters())  //Gradient cropping
      optimizer.step()  //Parameter update
      if epoch is a multiple of 5 and all images in I_train have been learned
        //Evaluation of images in I_val using current training network parameters
      then val_score←U-Net .eval(I_val)
        scheduler.step(val_score)  //Adjustment of network learning rates based on
                                   //assessment scores
    end
  end
end
return O
```

Fig. 7. The UNNN training algorithm.

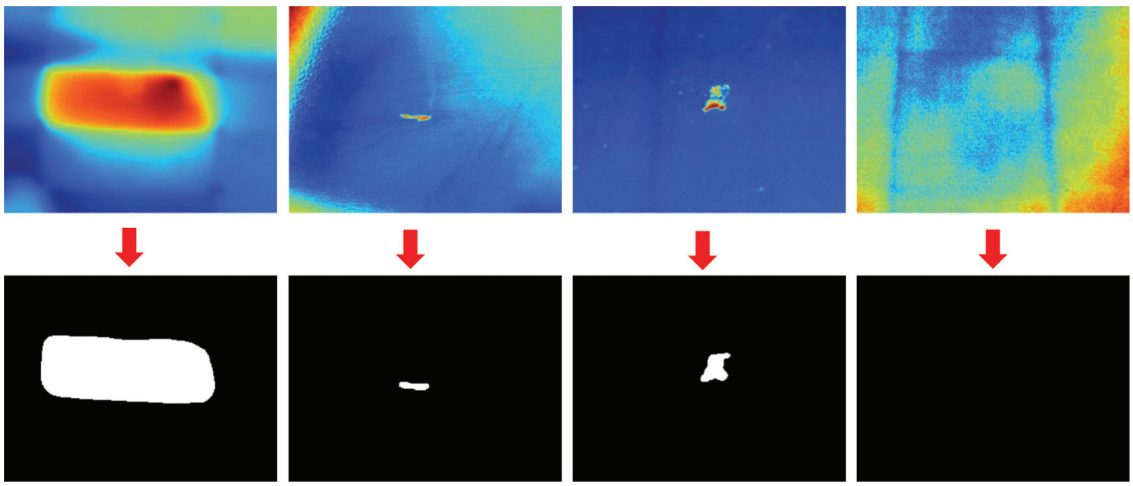

(a) Panel with power unit fault (b) Panel with safety-glass crack (c) Panel with contaminations (d) Panel without any defect

Fig. 8. Masks generated by the trained UNNN.

contour were also adopted to enhance the description of the geometric shape of the graph contour.

VI. FAULT DIAGNOSIS OF SPV PANELS

Given that SVM has demonstrated excellent performance in solving both binary and multi-class classification problems [19], an SVM-based smart technique will be developed in this section for diagnosing the health state of SPV panels. The input of the SVM will be the four defined graph contour features of the mask images generated by the trained UNNN. The output of the trained SVM will be four digital numbers 0, 1, 2, and 3, which respectively indicate the panel with a safety glass crack, the panel with safety glass contaminations, the panel with a power unit fault, and the healthy panel without any defect.

Then, the four features defined in Section V are extracted from 1,852 mask images. The calculation results will then be used as the input for training the SVM. The four features of the remaining 500 mask images are also calculated, and their results will be used to verify the trained SVM. In the SVM training process, in order to further improve the classification efficiency of the SVM, the above four features are fed into the SVM in different combination forms. As this study focuses on just four image features, for the sake of simplicity, their impact on image classification is roughly evaluated only through a trial-and-error approach. Nevertheless, when incorporating a larger set of image features into the classification process, a more rigorous scientific method, like significance calculation, should be employed to identify the most suitable features for assessing the health state of SPV panels. The classification accuracy rates of the SVM that are trained using different feature combinations are tabulated in Table III. Herein, it is worth noting that only four feature combinations with significant accuracy rates are listed in Table III, while those leading to unsatisfactory accuracy rates are not listed in the table for keeping a concise context of the paper.

From Table III, it is found that when the features of different combinations are used to train the SVM, the trained SVM shows different accuracy rates. The comparison has shown that higher accuracy rates, i.e., 80.9% and 81.2%, were achieved under the following two combinations:

- "contour perimeter" + "aspect ratio"
- "contour perimeter" + "aspect ratio" + "the ratio of contour area to the area of the outer rectangle"

Since a similar accuracy rate was obtained before and after considering "the ratio of contour area to the area of the outer rectangle," it suggests that this feature is not very helpful to improve the accuracy of the SVM.

In the meantime, from Table III, it is interestingly found that an accuracy of 80.9% is obtained when "contour perimeter" and "aspect ratio" are used in combination. However, after the "contour area" is added to the input, the accuracy of the SVM drops significantly down to 67.7%. In addition, an accuracy of 81.2% is obtained when "contour perimeter," "aspect ratio," and "the ratio of contour area to the area of the outer rectangle" are used in combination. However, after the "contour area" is added to the input, the accuracy of the SVM also drops significantly down to 67.7%. This suggests that the "contour area" has a negative influence on the accuracy of the SVM.

Therefore, by performing the above analysis, "contour perimeter" and "aspect ratio" are identified as the best feature combination for diagnosing the health state of SPV panels.

VII. CONCLUSIONS

By using the UNNN and SVM, a smart health state diagnosing technique was developed in this paper for assessing the health condition of SPV panels and thereby enhancing asset management in the SPPs. Through performing a systematic research, the following conclusions can be drawn:

- Since a fault can cause change in the temperature in the defective area on the surface of SPV panels, thermal infrared images, especially their mask images that contain minimal interference, are a reliable source for monitoring the health condition of SPV panels.
- SPV panel faults can be readily identified with reasonable accuracy by observing the graph contour characteristics in their thermal infrared images. Therefore, it is a feasible approach to diagnosing SPV panel faults by analyzing the graph contour features in the mask images deduced from their true color thermal infrared images.
- The UNNN, after being trained, is a proficient and reliable solution for image segmentation and producing mask images from the original color images.
- "contour perimeter" and "aspect ratio" are two ideal features that can be used by the trained SVM to assess the health state of SPV panels. By contrast, "contour area" has a negative influence on the accuracy of the SVM, and "the ratio of contour area to the area of the outer rectangle" has no significant influence on the classification accuracy of the SVM.

While the current study has yielded promising results, there remains a substantial amount of work that must be undertaken in the future to enhance the accuracy, reliability, and applicability of the techniques employed. Our forthcoming efforts will concentrate on several key aspects, including comparing our approach with other image

Table III. Classification accuracy of the SVM when using different feature combinations

	Combinations of the features			
	"contour area" + "contour perimeter" + "aspect ratio" + "the ratio of contour area to the area of the outer rectangle"	"contour area" + "contour perimeter" + "aspect ratio"	"contour perimeter" + "aspect ratio"	"contour perimeter" + "aspect ratio" + "the ratio of contour area to the area of the outer rectangle"
Accuracy	67.7%	67.7%	80.9%	81.2%

segmentation and classification techniques, enhancing the existing algorithms by leveraging their strengths, conducting a more extensive array of experiments, acquiring a greater number of thermal infrared images across diverse scenarios to expand our image database, and validating the improved methodology by implementing it for in situ monitoring of SPV panels within a SPP.

ACKNOWLEDGMENTS

The work reported above was supported by the Efficiency and Performance Engineering Network International Collaboration Fund (award No. of TEPEN-ICF2021-05).

CONFLICT OF INTEREST STATEMENT

The authors declare no conflicts of interest.

REFERENCES

[1] IEA, Solar PV, 2022. Available: https://www.iea.org/reports/solar-pv.

[2] IEA, Global Energy and Climate Model, 2022. Available: https://www.iea.org/reports/global-energy-and-climate-model.

[3] C. Toledo et al., "Measurement of thermal and electrical parameters in photovoltaic systems for predictive and cross-correlated monitorization," *Energies*, vol. 12, no. 4, p. 668, 2019.

[4] S. Daliento, A. Chouder, P. Guerriero, A. M. Pavan, A. Mellit, R. Moeini, and P. Tricoli, "Monitoring, diagnosis, and power forecasting for photovoltaic fields: a review," *Int. J. Photoenergy,* vol. 2017, 2017, Article ID 1356851. DOI: 10.1155/2017/1356851.

[5] F. Mallor et al., "A method for detecting malfunctions in PV solar panels based on electricity production monitoring," *Solar Energy*, vol. 153, pp. 51–63, 2017.

[6] E. García et al., "Solar panels string predictive and parametric fault diagnosis using low-cost sensors," *Sensors*, vol. 22, no. 1, p. 332, 2022.

[7] A. W. Kandeal et al., "Infrared thermography-based condition monitoring of solar photovoltaic systems: a mini review of recent advances," *Solar Energy*, vol. 223, pp. 33–43, 2021.

[8] Á. H. Herraiz, A. P. Marugán, and F. P. G. Márquez, "A review on condition monitoring system for solar plants based on thermography," in M. Papaelias, F. P. G. Márquez, and A. Karyotakis, *Non-Destructive Testing and Condition Monitoring Techniques for Renewable Energy Industrial Assets*, Butterworth-Heinemann 2020, pp. 103–118. DOI: 10.1016/B978-0-08-101094-5.00007-1.

[9] I. Segovia Ramirez, B. Das, and F. P. Garcia Marquez, "Fault detection and diagnosis in photovoltaic panels by radiometric sensors embedded in unmanned aerial vehicles," *Prog. Photovolt.: Res. Appl.*, vol. 30, no. 3, pp. 240–256, 2022.

[10] M. W. Akram et al., "Automatic detection of photovoltaic module defects in infrared images with isolated and develop-model transfer deep learning," *Solar Energy*, vol. 198, pp. 175–186, 2020.

[11] O. Ronneberger, P. Fischer, and T. Brox, "U-Net: convolutional networks for biomedical image segmentation," in *18th Int. Conf. Med. Image Comput. Comput.-Assist. Intervent. (MICCAI)*, Munich, Germany, Springer, LNCS, October 5–9, vol. 9351, pp. 234–241, 2015.

[12] C. Cortes and V. Vapnik, "Support-vector networks," *Mach. Learn.*, vol. 20, no. 3, pp. 273–297, 1995.

[13] S. Lu, B. T. Phung, and D. Zhang, "A comprehensive review on DC arc faults and their diagnosis methods in photovoltaic systems," *Renew. Sustain. Energy Rev.*, vol. 89, pp. 88–98, 2018.

[14] A. Bouraiou et al., "Experimental investigation of observed defects in crystalline silicon PV modules under outdoor hot dry climatic conditions in Algeria," *Solar Energy*, vol. 159, pp. 475–487, 2018.

[15] X. Wang, W. Yang, B. Yang, K. Wei, Y. Ma, and D. Zhang, "Intelligent monitoring of photovoltaic panels based on infrared detection," *Energy Rep.*, vol. 8, pp. 5005–5015, 2022.

[16] D. Pillai and N. Rajasekar, "A comprehensive review on protection challenges and fault diagnosis in PV systems," *Renew. Sustain. Energy Rev.*, vol. 91, pp. 18–40, 2018.

[17] M. Arani and M. Hejazi, "The comprehensive study of electrical faults in PV arrays," *J. Electr. Comput. Eng.*, vol. 2016, p. 8712960, 2016.

[18] O. Ronneberger, P. Fischer, and T. Brox, *U-Net: Convolutional Networks for Biomedical image Segmentation*. Cham: Springer, 2015.

[19] Z. Long et al., "Recognition and classification of wire bonding joint via image feature and SVM model," *IEEE Trans. Comp. Packaging Manuf. Technol.*, vol. 9, no. 5, pp. 998–1006, 2019.